JATIS Journal of Astronomical Telescopes, Instruments, and Systems

RESEARCH PAPER

Milky Way and nearby galaxy science with the SALTUS space observatory

Rebecca C. Levy[a,*] **Alexander Tielens**[b,c] **Justin Spilker**[d] **Daniel P. Marrone**[a] **Desika Narayanan**[e,f] **and Christopher K. Walker**[a]

[a]University of Arizona, Department of Astronomy and Steward Observatory, Tucson, Arizona, United States
[b]Leiden Observatory, Leiden, The Netherlands
[c]University of Maryland, Astronomy Department, College Park, Maryland, United States
[d]Texas A&M University, George P. and Cynthia Woods Mitchell Institute for Fundamental Physics and Astronomy, Department of Physics and Astronomy, College Station, Texas, United States
[e]University of Florida, Department of Astronomy, Gainesville, Florida, United States
[f]University of Copenhagen and DTU-Space, Technical University of Denmark, Cosmic Dawn Center at the Niels Bohr Institute, Kongens Lyngby, Denmark

ABSTRACT. We present an overview of the Milky Way (MW) and nearby galaxy science case for the Single Aperture Large Telescope for Universe Studies (SALTUS) far-infrared (IR) NASA probe-class mission concept. SALTUS offers enormous gains in spatial resolution and spectral sensitivity over previous far-IR missions due to its cold (<40 K) 14-m primary mirror. Key MW and nearby galaxy science goals for SALTUS focus on understanding the role of star formation in feedback in the local universe. In addition to this science case, SALTUS would open a new window to galactic and extragalactic communities in the 2030s, enabling fundamentally new questions to be answered, and would be a far-IR analog to the near- and mid-IR capabilities of the James Webb Space Telescope. We summarize the MW and nearby galaxy science case and plans for notional observing programs in both guaranteed and guest (open) times.

 [DOI: 10.1117/1.JATIS.10.4.042304]

Keywords: mission concept; galactic science; extragalactic science; terahertz spectroscopy; far-infrared; heterodyne resolution

Paper 24049SS received Apr. 22, 2024; revised Jul. 12, 2024; accepted Aug. 13, 2024; published Sep. 13, 2024.

1 Introduction

The Single Aperture Large Telescope for Universe Studies (SALTUS) observatory is a far-infrared (FIR) mission concept proposed to NASA's recent astrophysics probe explorer call for proposals.[1] Its unique 14-m primary mirror and sensitive FIR ($\approx 30-700\ \mu$m) instrumentation would provide orders-of-magnitude improvements over past and other proposed FIR space missions. The very large primary mirror size results in unprecedented $\sim 1''$ spatial resolution in the FIR, making SALTUS a well-matched bridge in wavelength between the James Webb Space Telescope (JWST) and the Atacama Large Millimeter/submillimeter Array (ALMA). The overall telescope, receivers, and spacecraft architectures are described in detail in a series of papers elsewhere in this issue.[2–6] Briefly, the two instruments planned for SALTUS are SAFARI-Lite and HiRX. SAFARI-Lite is a direct detection spectrometer providing medium resolution ($R \sim 300$) spectroscopy over the entire 34 to 230 μm wavelength range simultaneously.[5] HiRX

*Address all correspondence to Rebecca C. Levy, rebeccalevy@arizona.edu

2329-4124/2024/$28.00

is a multi-pixel, multi-band heterodyne receiver ($R \sim 10^5 - 10^7$) enabling sub-km s^{-1} spectroscopy of key spectral lines for interstellar medium (ISM) science.[6]

This paper provides an overview of the Milky Way (MW) and nearby galaxy science uniquely enabled by SALTUS. Accompanying papers in this issue describe the capabilities of SALTUS for high-redshift galaxies,[7] star and planet formations,[8] and solar system observations.[9] In the remainder of this section, we provide background on the key principles and tracers of processes in the ISM of galaxies and the MW. Section 2 highlights the SALTUS performance characteristics most relevant for MW and nearby galaxy science. In Sec. 3, we present several key measurements, enabled by SALTUS, that answer key open questions in the fields of MW and nearby galaxy science.

1.1 Key Cosmic Ecosystems Questions

The 2020 Astronomy Decadal Survey[10] laid out a number of key science questions pertaining to our *cosmic ecosystem* that drive the science priorities for the next decade and beyond. Although the capabilities of SALTUS would enable substantial progress toward the majority of the cosmic ecosystem questions, here, we focus on the following key decadal questions (DQs) as they pertain to observing the ISM of the MW and nearby galaxies.

1. How do star-forming structures arise from, and interact with, the diffuse interstellar medium?
   (a) How does injection of energy, momentum, and metals from stars ("stellar feedback") drive the circulation of matter between phases of the ISM and circumgalactic medium?
2. What regulates the structures and motions within molecular clouds?
   (b) What is the origin and prevalence of high-density structures in molecular clouds, and what role do they play in star formation?
   (c) What generates the observed chemical complexity of molecular gas?
3. How do gas, metals, and dust flow into, through, and out of galaxies?
   (d) The production, distribution, and cycling of metals.
   (e) The coupling of small-scale energetic feedback processes to the larger gaseous reservoir.
4. How do the histories of galaxies and their dark matter halos shape their observable properties?
   (f) Connecting local galaxies to high-redshift galaxies.
   (g) The evolution of morphologies, gas content, kinematics, and chemical properties of galaxies.

1.2 Stellar Feedback and the Ecology of Galaxies

Stellar feedback plays a central role in galactic ecology (Fig. 1) and is a key question posted in the 2020 Astronomy Decadal Survey (e.g., DQs 1 and 3). During their formation phase, protostellar jets and winds stir up their environment and greatly modify the structure of the clouds in which they form and hence the star formation process. During their main sequence phase, the interaction of massive stars with their environments regulates the evolution of galaxies (DQs 1a and 3b). Mechanical and radiative energy input by massive stars stir up and heat the gas and control cloud and intercloud phases of the ISM. The dominant mode of stellar feedback changes with the stellar/cluster mass and as the star/cluster evolves.[11–13] Stellar feedback also governs the star formation efficiency of molecular clouds.[11,14–16] On the one hand, stellar feedback can lead to shredding of the nascent molecular cloud within a few cloud free-fall times, thereby halting star formation.[17–19] On the other hand, massive stars may also provide positive feedback to star formation as gravity can more easily overwhelm cloud-supporting forces in swept-up compressed shells.[20,21] The Spitzer/GLIMPSE galactic plane survey has revealed hundreds of parsec scale bubbles associated with O and B stars, attesting to the importance of stellar feedback in stirring

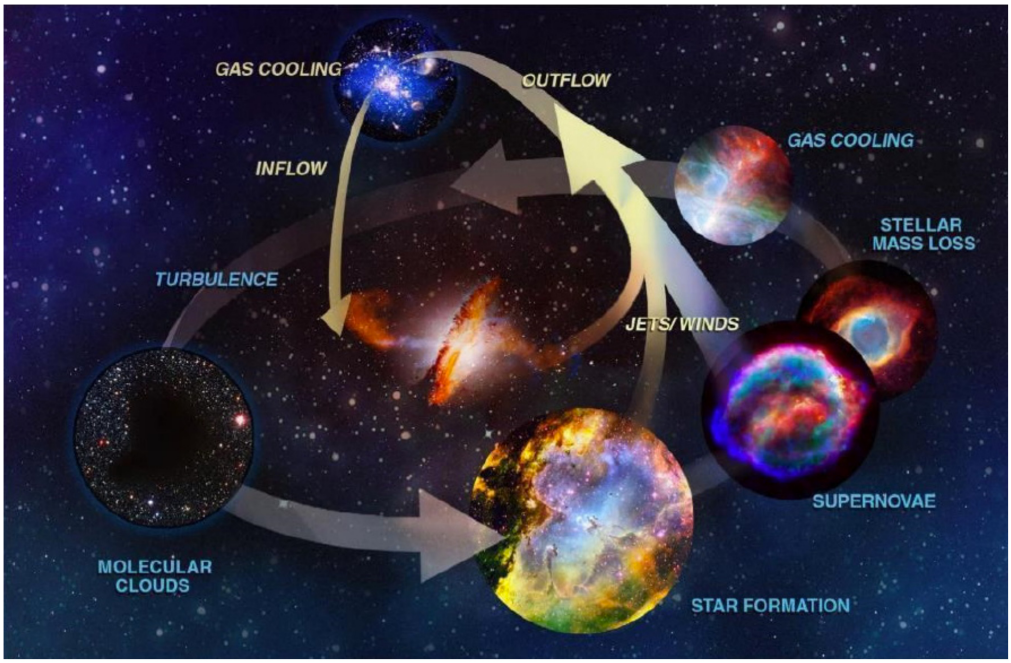

Fig. 1 Role of feedback and the lifecycle of galaxies. Stars form inside dense clouds. The mechanical and radiative energy injected during their evolution from the protostellar to the main sequence to the supernova phase will heat interstellar gas, inject turbulence into the medium, disrupt molecular clouds, and create the various phases of the ISM. During the asymptotic giant branch and the supernova phases, newly synthesized elements will be ejected, slowly enriching the ISM. The concerted action of massive stars in rich OB associations will drive the formation of chimneys that vent enriched gas into the lower halo and even the intergalactic medium. Halo gas will condense in clouds that rain back onto the galactic plane. The concerted action of these processes drives the evolution of galaxies. The figure is taken from Ref. 10. SALTUS will enable key measurements across the feedback and life cycle at unprecedented spatial and spectral resolutions.

up the ISM.[22] The expansion of these bubbles may be driven by the thermal pressure of the warm ionized gas, radiation pressure by stellar photons, or mechanical energy input by stellar winds.[12,23,24] The PHANGS survey revealed larger (up to ≈1 kpc) bubbles in nearby galaxies, likely driven by mechanical energy from stellar winds and (clustered) supernovae.[25,26] As massive star formation dominates the energetics and feedback in star-forming galaxies, properly accounting for the star formation feedback is a critical ingredient of galaxy evolution models, and validating the subgrid feedback descriptions in these hydrodynamic studies is of paramount importance.[27–30]

1.3 Tracers of the ISM

Much of the interaction of massive stars with their environment occurs in regions shrouded in dust, and the far-infrared—where dust extinction is minimal—provides many key diagnostic transitions that measure the physical conditions in these regions and trace their evolution. Specifically, this spectral range hosts atomic and ionic fine-structure transitions, covering a wide range in critical density (100 to 500 K; $3 \times 10^2 - 3 \times 10^4$ cm^{-3}).[23]

During the protostellar and main sequence phases, mechanical energy input by stars drives strong shock waves into the surrounding gas, sweeping it up in dense shells. The far-infrared provides a convenient probe of the temperature structure through the slew of CO pure rotational transitions accessible with SAFARI-Lite and HiRX.[31] The chemical processing of the gas by the shock starts with the sputtering of ice mantles dominated by H_2O and to a lesser extent NH_3. This is the first step in the build-up of chemical complexity in regions of star formation (DQs 2b, 3a, 4b).

The physical conditions in photodissociation regions (PDRs) can be studied through the [OI] 63 and 145 μm, [CII] 158 μm, and [SiII] 35 μm fine-structure transitions, as well as high-J CO rotational transitions (e.g., $J = 10 - 9$ at 260 μm through $J = 19 - 18$ at 137 μm), in addition to ^{13}CO isotopes and the deuterated hydrogen (HD) molecule. The high sensitivity will bring many higher-order CO transitions into SALTUS' purview as well. All of these transitions are known to be bright in PDRs.[32–34] Together, these transitions span a wide range in critical densities ($\simeq 3 \times 10^3 - 10^6$ cm^{-3}) and excitation energies ($\simeq 100 - 500$ K) and thus provide powerful tools to determine physical conditions in these neutral gas regions. The strong far-UV irradiation of PDRs also leaves its imprint on the chemical composition, leading to a strong stratification of the molecular composition ranging from a surface layer characterized by small hydride radicals to the deeper zones dominated by heavier species, including CO and HCN.[35] The first steps toward molecular complexity start with the formation of simple hydride radicals (DQ 2b). Because of their large moments of inertia, light hydride radicals have their main transitions in the far-IR. Herschel detected strong emission from HD, OH, H_2O, H_2O^+, H_3O^+, CH, CJ^+, SH, HF, and H_2Cl^+ in the Orion Bar.[36]

Finally, the [NeIII] 36 μm, [SIII] 33.4 μm, [NII] 122 and 205 μm, [NIII] 57 μm, and [OIII] 52 and 88 μm lines trace ionized gas in HII regions around hot young stars and provide a measure of the gas density and the hardness of the stellar radiation fields.[37] Importantly, these transitions are not temperature sensitive. Therefore, galactic elemental abundance gradients (DQ 4b) can be accurately assessed by combining measurements of these species in the far-IR with mid-IR neutral hydrogen recombination lines provided by JWST.

2 SALTUS Performance for MW and Nearby Galaxy Science

The SALTUS telescope, instrumentation, and spacecraft design principles are described in detail in accompanying papers in this issue;[1–6] here, we briefly describe the performance metrics most relevant for the MW and nearby galaxy science community. We envision that the SAFARI-Lite grating spectrometer will be the workhorse instrument for this community. In addition, key spectral lines (e.g., water, [CII]) will be observable with the HiRX heterodyne instrument at a very high spectral resolution.

2.1 Wavelength Coverage

The SAFARI-Lite instrument[5] provides $R \approx 300$ ($\Delta v \approx 1000$ km s^{-1}) spectroscopy over the entire 34 to 230 μm wavelength range simultaneously, covering the entire FIR at $z = 0$ (Fig. 2). To achieve this, the wavelength range is divided into four co-aligned bands. Light enters the instrument through six spatial pixels (arranged linearly on-sky), which are then dispersed onto 180-detector MKID arrays. ISM heating and cooling are governed by forbidden transitions of atoms and molecules that occur in the FIR. The key line, and the brightest line in galaxies in the FIR, is the 158 μm transition of [CII]. This line will be covered by both SAFARI-Lite and HiRX, enabling detection and characterization over a range of environments and targeted high spectral resolution kinematic/energetic studies. Other key lines covered by SAFARI-Lite include [SIII] 34 μm, [SiII] 35 μm, [OI] 63,145 μm, [OIII] 52,88 μm, [NII] 122,205 μm, and high-J CO transitions (Fig. 2).

The HiRX instrument[6] provides sub-km s^{-1} spectral resolution in four tunable bands chosen to cover key spectral features for a broad range of science cases (Fig. 2). Band 1 (521 to 659 μm) covers two key CO rotational transitions ($J = 5 - 4$ and $J = 4 - 3$) and an H_2O ortho transition. Band 2 (136 to 273 μm) covers key lines such as [NII] 122,205 μm, [OI] 145 μm, [CII] 158 μm, several deuterated water (HDO) transitions, two prominent H_2O lines, and several high-J CO lines. Band 3 (112 μm) covers the ground state rotational transition of deuterated molecular hydrogen (HD 1-0). Band 4 (56.2, 63.2 μm) covers HD 2-1 and [OI] 63 μm.

2.2 Spatial Resolution

It is expected that SALTUS would be diffraction limited down to 30 μm, achieving 0.5 to 3.6″ resolution over the wavelength range covered by SAFARI-Lite and 0.8 to 9.7″ resolution over the HiRX bands (Fig. 2). As a result, SALTUS will offer transformative gains in physical resolution for the study of the MW and nearby galaxies compared with the Herschel Space

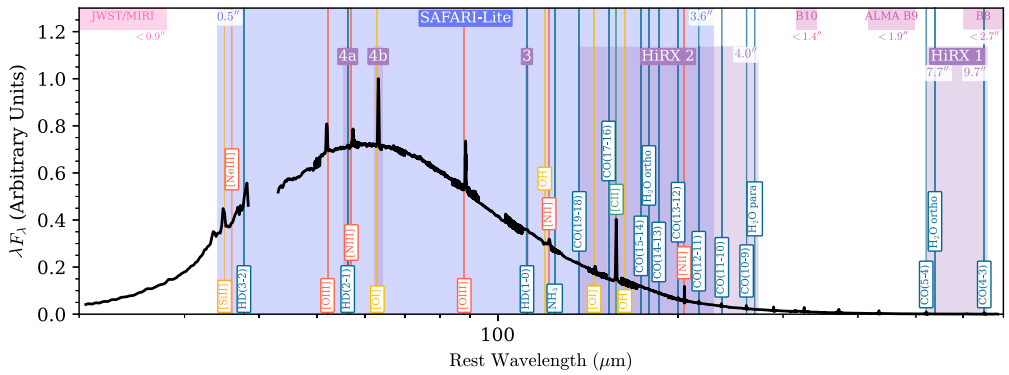

Fig. 2 Example of the wavelength coverage of SALTUS compared with a spectrum of the archetypal nearby starburst galaxy M 82 (black; from Spitzer/IRS,[38] ISO/LWS,[39] and Herschel/SPIRE[40]). The SAFARI-Lite simultaneous coverage is shown in blue and the HiRX bands are shown in purple. The coverage of JWST/MIRI (light pink) and the ALMA bands (dark pink) are plotted for reference. The angular resolutions of each instrument at key wavelengths are shown in the corresponding colors. Key diagnostic lines are shown, tracing the ionized (red), neutral (yellow), molecular (blue), ionized/neutral (orange), and ionized/neutral/molecular (green) ISM phases; this list is not exhaustive. With SALTUS, we will measure spectra of nearby galaxies at substantially higher spatial resolution, spectral resolution, and sensitivity compared with previous instruments, opening a fundamentally new window into the study of the ISM in the local universe.

Observatory (≈16× smaller beam area) or the Stratospheric Observatory for Infrared Astronomy (SOFIA, ≈30× smaller beam area). For example, SALTUS will enable the mapping of MW sources, such as Orion BN/KL at ≈200 to 1000 AU spatial resolution, filling gaps between ISM and star and planetary system formation science questions. For galaxies within 20 Mpc (e.g., the PHANGS sample[41,42]), SALTUS enables mapping of entire galaxies on 50 to 200 pc scales, revealing the structure of the ISM and sites of feedback. As indicated in Fig. 2, the spatial resolution achieved by SALTUS is extremely well-matched to JWST/MIRI (≈ 0.9″ at 28 μm) and ALMA (<1.4″ at 345 μm; <2.7″ at 650 μm).

2.3 Mapping Sensitivity

SALTUS' large (14 m), passively cooled (<40 K) primary mirror offers transformative increases in sensitivity over previous instruments.[1] The sensitivity of SAFARI-Lite is similar to or better than that of JWST/MIRI at the short wavelength end and ALMA at the long wavelength end. SAFARI-Lite would be more than two orders of magnitude more sensitive compared with previous comparable instruments, such as the Photodetector Array Camera (PACS) on Herschel[43] and Field-Imaging Far-Infrared Line Spectrometer (FIFI-LS) onboard SOFIA.[44]

2.4 Spectral Mapping Speed

Although SALTUS has a large primary mirror, it is able to map a ≈5 arcmin^2 area without repointing using a fine-steering motor. This map size is similar to those of single JWST/NIRCam and MIRI images. Crucially, however, these "maps" from SALTUS/SAFARI-Lite are three-dimensional, containing a spectrum covering 34 to 230 μm at each pixel and therefore contain significantly more information than single filter images from JWST. This mapping area is sufficient to capture MW star-forming regions and many nearby galaxies in one or two pointings. Larger, more nearby targets, e.g., M 82, NGC 253, or local group galaxies, will need multiple pointings to observe the entire disk, but a single pointing is sufficient to study particular areas of interest (e.g., galactic centers and regions of high star formation).

3 Key MW and Nearby Galaxy Science Goals for SALTUS

SAFARI-Lite's high spatial resolution and simultaneous 34 to 230 μm full spectral coverage, combined with HiRX's sub-km s^{-1} spectral resolution and efficient mapping capabilities using a scanning mirror, make SALTUS the only observatory that can measure the key diagnostic lines of gas; quantitatively address the roles of stellar feedback in the evolution of regions of massive

star formation and of protostellar feedback during the earliest, deeply embedded phases of star formation; and determine how this depends on the cluster characteristics and core environment (e.g., Fig. 1). Here, we present some sample science use cases that address the key DQs laid out in Sec. 1.1.

3.1 Understanding the Role of Feedback in MW Star-Forming Regions

A key SALTUS science goal aims to understand the role of feedback in star-forming regions, both in nearby MW regions as well as in nearby spiral galaxies. It quantifies the kinetic energy and momentum input during the earliest, deeply embedded phases of star formation and addresses how this depends on the cluster characteristics and core environment (DQs 1a, 3b, 4b).

Orion BN/KL and NGC 1333 are the two prototypical galactic sources of star formation to be studied that demonstrate SALTUS' unique capabilities to study protostellar outflows to the general community. The combination of high spatial resolution, simultaneous full spectral coverage, and mapping efficiency make SALTUS the only observatory that can measure the key diagnostic lines of interstellar gas and quantitatively address the role of protostellar feedback during the earliest, deeply embedded phases of star formation, as well as how this depends on the cluster characteristics and core environment (DQ 1a and 3b). ALMA can measure low J CO sub-millimeter transitions at a high spatial resolution, but the high J transitions that are key to measuring the temperature, density, and column density of warm, dense shocked gas that occurs at far-IR wavelengths are only accessible with SALTUS (DQ 2a). JWST/MIRI can measure the pure rotational transitions of H_2 in the mid-IR, which are good diagnostics of the shock characteristics as well. However, the small footprint of MIRI spectroscopy (<7.7″) precludes efficient mapping of regions of extended emission associated with protostellar outflows. Another probe of these outflows can be achieved through spectral mapping in key diagnostic lines of J and C shocks ([OI], H_2O, high J CO) using SAFARI-Lite and HiRX, which probes a range of cluster characteristics and molecular core properties.[45–47]

The BN/KL region in Orion is the nearest site of massive star formation, presenting an excellent opportunity to study in detail the interaction of massive protostars with the surrounding molecular core (DQs 1a and 3b). Scaling the Herschel/PACS fluxes for peak 1,[48] assuming homogeneous emission, results in expected line fluxes in the 1 to 3″ SALTUS beam of 3×10^{-18} to 2×10^{-15} W m^{-2} for selected ^{12}CO, H_2O, and OH lines and the [OI] 63 μm fine-structure line. In ^{13}CO, SALTUS can be expected to detect lines as high as $J = 30 - 29$ ($E_u \sim 2500$ K). SAFARI-Lite can map the 5 arcmin^2 of peaks 1 and 2 in Orion down to a limiting line flux of $1 - 3 \times 10^{-18}$ W m^{-2} in 5 h. This data can be analyzed to determine the column density, preshock density, and shock velocity[48] on a 1 to 3″ scale and quantify the disruption of the Orion Molecular Cloud (OMC) 1 core by this explosion and its effect on the surrounding star cluster.

NGC 1333 is the most active region of low-mass star formation in the Perseus molecular cloud, containing a large-membership (>100) young clusters, and it is considered the prototypical, nearby (135 pc) cluster-forming region.[49,50] NGC 1333 contains many molecular outflows (Fig. 3)[56–58] that appear capable of maintaining turbulence and therefore limiting the rate of star formation.[59–61] Typical Herschel/PACS high-J CO and H_2O line fluxes of the shock emission associated with the protostellar outflows in NGC 1333 are $\sim 10^{-16}$ W m^{-2}[62] and translate into average line fluxes of 6×10^{-18} W m^{-2} in the SALTUS beam. A spectral-spatial study with SAFARI-Lite can map a 1 arcmin^2 and detect these lines at an S/N ratio of 30. Spitzer/IRS H_2 studies[63] imply that the shocked gas comprises in total some 5 arcmin^2. A fully sampled 34 to 230 μm spectral-spatial map of the shocked gas in NGC 1333 takes 5 h with SAFARI-Lite. These data can be analyzed analogously to the Herschel data using existing shock models, provide on a ∼3″ scale size the shock characteristics (preshock density, shock temperature, and shock velocity), and quantify the energy and momentum provided by the protostellar outflows for the NGC 1333 cluster (DQs 1a and 3b). A combination of these data with ground-based interferometric maps in complex organic molecules can then address the influence of shocks on the organic inventory of star-forming cores (DQs 2b and 3a).

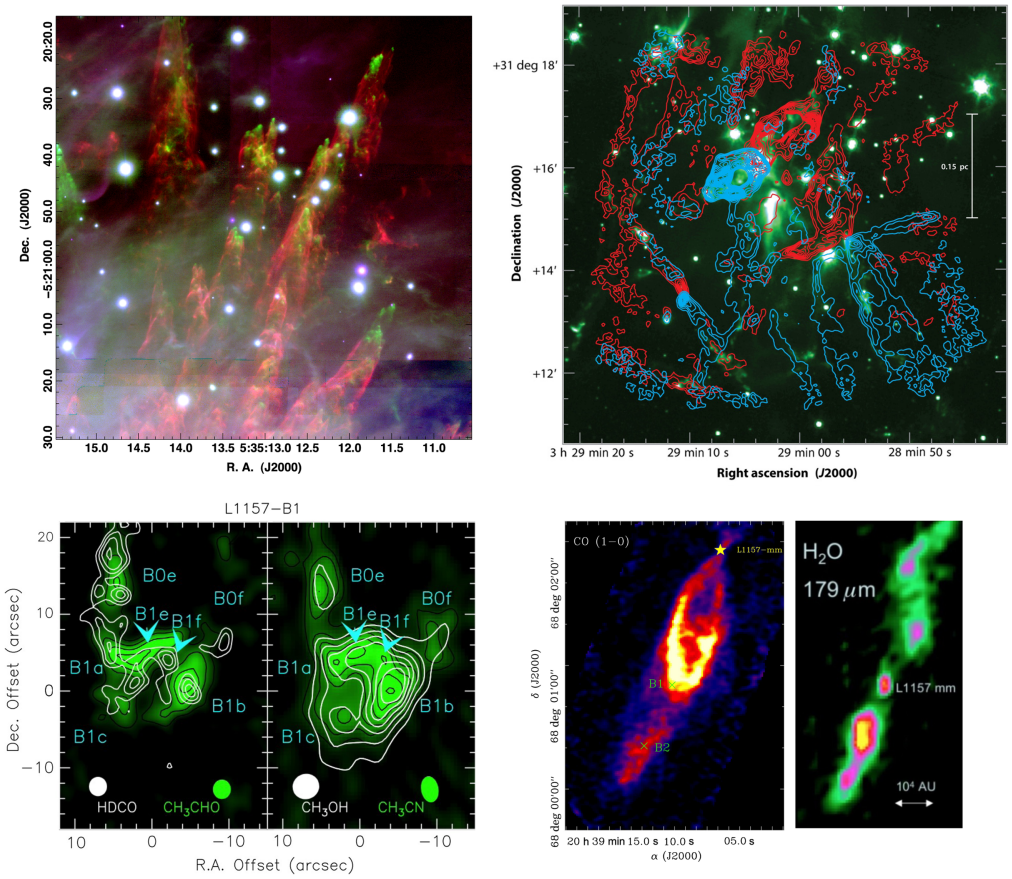

Fig. 3 Top row: (Left) part of the Northern (peak 1) outflow lobe in the BN/KL region as traced in the *K* band (blue), 1.644 μm [FeII] (green), and 2.122 μm H_2 (red), revealing well-defined H_2 emission with [FeII] fingertips.[51] (Right) Outflows driven by the young stellar cluster in the NGC 1333 region. Some 22 outflow lobes are evident in the 4.5 μm IRAC image (green) and the red and blue shifted CO $J = 1 - 0$ emission in this 0.5 pc field.[52] Bottom row: the bipolar outflow associated with the protostar L1157 mm. (Right) H_2O emission in the ground-state ortho line at 179 μm obtained by Herschel/PACS at a resolution of 13″, revealing unresolved emission clumps.[53] (Middle) A blow-up of the blue shifted southern lobe in the CO $J = 1 - 0$ transition at a resolution of 3″. Two bright emission structures, B1 and B2, are indicated.[54] (Left) Interferometric studies of molecular emission in the B1 clump break this structure into multiple components.[55] Green contours trace acetaldehyde and methyl cyanide, respectively, and white is deuterated formaldehyde and methanol. The clear chemical differentiation of these complex organic molecules reflects the effects of the interplay of shock sputtering of icy grains and subsequent chemistry in the warm gas. Beam sizes (~3″) are indicated and comparable to SAFARI-Lite at the longest wavelengths.

3.2 Understanding the Role of Feedback in Nearby Galaxies

The second part of this science case bridges "ground-truth" observations of feedback on the scale of individual MW star-forming regions to the spatially unresolved view of galaxy evolution throughout the distant universe (DQ 4a). Energetic feedback from star formation processes, the lives and deaths of stars, and nuclear black holes [or active galactic nuclei (AGN)] are critical factors in the growth and evolution of galaxies and the gas that surrounds them. The effects of feedback are multiscale, ranging from individual stars and clusters to galaxy-scale outflows extending several kiloparsecs into the circumgalactic medium. However, the injection sites of feedback are small-scale, originating from individual supernovae, star clusters, and near the AGN itself (Fig. 4).

Spectral line strengths and ratios (e.g., [SiII] 35 μm, [OI] 63, 145 μm, [OIII] 52, 88 μm, and [NII] 122, 205 μm) are used as diagnostics of the radiation field, temperature, and/or density to characterize shocks and feed-back in the ISM, especially when coupled with modeling codes

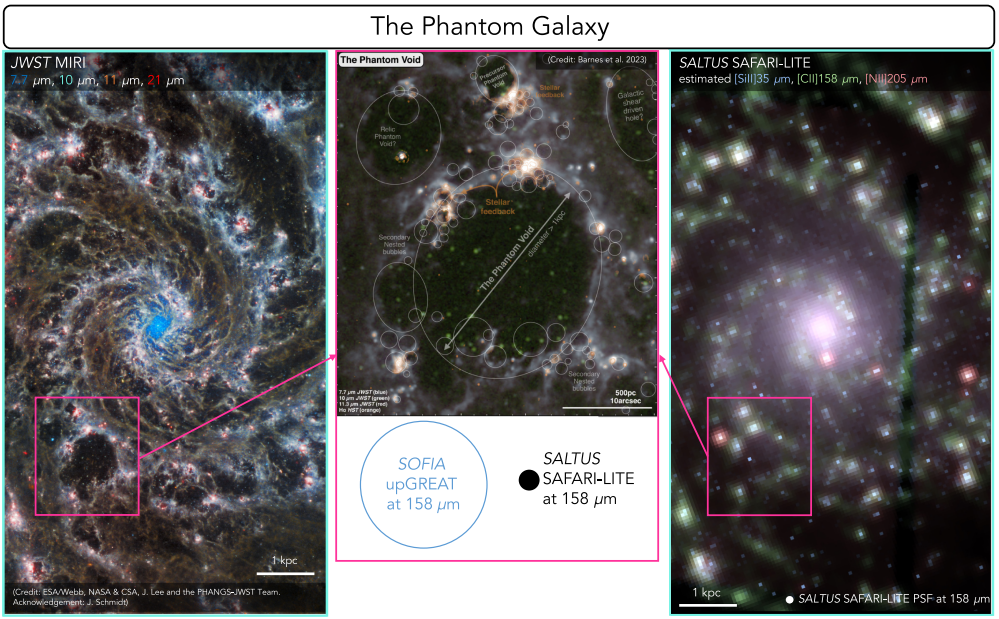

Fig. 4 JWST has revealed new details in the structure of the interstellar medium (ISM) by observing the dust emission of NGC 628. (Left) The concerted action of stellar winds and supernovae create superbubbles, typically <500 pc across, that drive the evolution of the galactic ecosystem (image credit: ESA/Webb, NASA, and CSA, J. Lee, and the PHANGS-JWST Team). (Center) SALTUS will complement these JWST studies, extending high-resolution observations of the ISM into the FIR (image credit[26]). (Right) As the simulated SAFARI-Lite image illustrates, SALTUS will simultaneously measure key diagnostic atomic fine-structure lines such as the three simulated here, resolving these bubbles and quantifying the physical conditions and energetics of this feedback.

such as CLOUDY.[64] The [CII] line at 158 μm is a tracer of the neutral ISM, photodissociation regions, and star formation.[65–67] [CII] and [OI] 63 μm are major cooling channels for the ISM. The [OIII] and [NII] lines are tracers of ionized gas in the HII regions and the diffuse ISM, respectively. Because FIR lines largely govern the bulk heating and cooling of the ISM, they are key to understanding the energy balance in the ISM, especially in regions of active feedback.

Figure 4 gives an example of a nearby, star-forming galaxy M 74 (The Phantom Galaxy or NGC 628). Although new observations from JWST have resolved the galaxy and sites of stellar feedback in stunning detail (Fig. 4),[25,26,42] the physics of the photodissociation regions surrounding these supernova bubbles is unknown without FIR diagnostics. Understanding how ISM heating and cooling vary under such conditions requires high spatial resolution observations of key FIR diagnostics (DQ 1a and 4b). SAFARI-Lite enables such detailed studies of the effects of stellar and AGN feedback across a suite of nearby galaxies. The capabilities are highlighted in Fig. 4 (right), showing the anticipated [CII] and [NII] 205 μm emission from M 74 at SAFARI-Lite resolution. The [CII] emission is estimated from the continuum-subtracted 3.3 μm PAH feature,[68] and the [NII] emission is based on Hα.[69] A 100σ detection of the [CII] 158 μm line (to enable robust detection of weaker lines and continuum) over the full $9' \times 9'$ extent of M 74 requires 12 h.

HiRX enables high spectral resolution ($R > 10^6$, $\Delta v < 1$ kms^{-1}) observations of strong emission lines (e.g., [CII] 158 μm, [NII] 205 μm, [OI] 145 μm, H_2O, several high-J CO lines; Fig. 2). The precision kinematics yield robust measurements of energy and momentum injection from feedback and shocks on scales ranging from star clusters to large-scale outflows[70,71] (DQs 1a, 3a, 4b). In M 74 specifically (Fig. 4), the expansion of the "Phantom Void" is 15 to 50 km s^{-1}. HiRX will be the only instrument capable of spatially and spectrally resolving feedback-driven bubbles, which are expected to be commonplace in star-forming galaxies.[25,26]

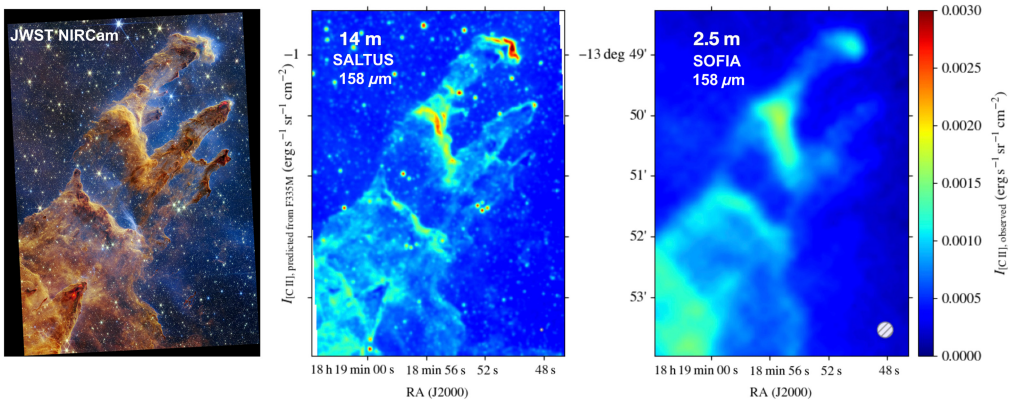

Fig. 5 Simulated SALTUS image at 2.5″ angular resolution (middle) of the [CII] 158 μm emission in NGC 6611 (Pillars of Creation) is similar to the JWST NIRCam image (left) and compared with the SOFIA-created map[72] (right). SAFARI-Lite can map this 10 arcmin^2 region in 10 h and simultaneously provide maps in all diagnostic lines and photo-dissociation regions (PDRs) and HII regions in our galaxy and the local group probing the physical environment produced by radiation feedback of massive stars and its link to stellar clusters and its molecular core.

3.3 Example Community Science: Stellar Feedback in Regions of Massive Star Formation

This topic aims to understand the role of stellar feedback in regions of massive star formation: How much kinetic energy is contributed to the ISM, how does this depend on the characteristics of the region, and in connection to this, how does the surrounding medium react (DQ 1a, 2a, 3b, 4b)? This objective is addressed by spectral-spatial mapping of regions of massive star formation in the dominant far-IR cooling lines of PDR gas using both the SAFARI-Lite and HiRX instruments (c.f., Pillars of Creation in Fig. 5). The sample consists of 25 regions with typical sizes of 25 arcmin^2, covering a range in stellar cluster properties (single stars to small clusters to super-star clusters), GLIMPSE bubble morphology (ring-like, bi- or multi-polar, complex), environment (isolated star-forming region, galactic mini starburst, and nuclear starburst), and cluster age (0.1 to 5 Myr).

SAFARI-Lite will provide full spectra over the 34 to 230 μm range, containing the key diagnostic atomic fine-structure transitions. SOFIA/upGREAT studies of the [CII] 158 μm emission of regions of massive star formation have demonstrated the feasibility of this technique.[73,74] Together, these two datasets quantify the kinetic energy of the expanding shell as well as the thermal, turbulent, and radiation pressures on the shell that can be directly compared with radiative and mechanical energy inputs of the stellar cluster.

3.4 Example Community Science: Putting Early-Universe Feedback in Context with Local Analogs of the First Galaxies

The first year of JWST observations revealed that early generations of galaxies were typically much lower in mass and significantly less metal-enriched compared with the massive star-forming spiral galaxies that dominate star formation today. Consequently, their UV radiation fields were harder,[75] which impacted the gas ionization state and cooling rate. The shallow gravitational potential wells also enhanced the effects of supernova-driven feedback as single supernovae could eject up to ~95% of the heavy elements formed during the star's lifetime into the circumgalactic medium.[76,77] Although ALMA now allows the key far-IR fine structure diagnostic lines (e.g., [CII], [OIII]) to be detected at high redshifts, these lines still take several hours to detect even in the most massive and UV-luminous reionization-era galaxies[78] and are generally out of reach for the more typical galaxies thought to drive cosmic reionization.

Due to community efforts, many nearby galaxy populations bearing similarities to UV-bright reionization-era galaxies in terms of their mass, metallicity, and harsh UV radiation fields have been identified. Though rare locally and largely unknown during the time of Herschel, these low-redshift galaxies are plausible analogs to early star-forming galaxies. Such local low-metallicity dwarf galaxies are natural extensions to the SALTUS low-redshift GTO efforts to measure and

resolve the injection of feedback energy on small spatial scales far beyond the capabilities of Herschel[79] or a 1 m-class FIR mission. With the same observables as the GTO program of star-forming spirals and starbursts and the most commonly detected lines found with ALMA at high redshifts, SALTUS enables ∼200 pc-scale maps of the FIR fine-structure lines and underlying dust continuum in low-redshift analogs of the first generation of galaxies (DQs 1a, 3b, 4a, 4b).

3.5 Example Community Science: Spectral Line Survey

The benefits of performing high-frequency spectral line surveys were recognized and exploited by Herschel HIFI, which resulted in the first reported detections of SH^+, HCl^+, H_2O^+, and H_2CL^+.[80–82] The formation of these small hydrides typically represents the first step in gas phase chemistry routes toward molecular complexity in space (DQ 2b). However, the spectral surveys with HIFI were severely limited by sensitivity. SALTUS' increased aperture results in a 16× increased sensitivity for these unresolved sources and can be expected to lead to an enhanced line density and discovery space (DQ 4b). Moreover, the wavelength coverage of SALTUS bridges the gap between spectral line surveys to be carried out with JWST/MIRI and ALMA.[83]

4 Conclusions

Unlocking the details of ISM heating and cooling, feedback, and star formation as a function of the environment are keys to understanding our cosmic ecosystem[10] and rely on measurements that can only be made in the FIR. Although any future FIR facility will offer transformative gains over previous observatories at this wavelength, only SALTUS will enable the spatially resolved studies in nearby galaxies to probe a wider range of conditions and to inform numerical simulations. Priority MW measurements include measuring PDRs and feedback in prototypical high- and low-mass star-forming regions at unprecedented resolution and sensitivity, bridging the gaps between studies of star and planet formation and the ISM. In nearby galaxies, the priority is to measure PDRs and feedback in well-characterized prototypes (e.g., M 74) across a range of environments. SALTUS' transformative increase in spatial resolution, spectral coverage, and sensitivity at these wavelengths ensures that it will be responsive to the needs of and bridge gaps between the galactic and nearby extragalactic communities of the 2030s. No other FIR facility will provide such seamless continuity in our understanding of the ISM after a decade of JWST observations and ALMA/ALMA-2030.

Disclosures

The authors have no relevant financial interests in the manuscript nor do they have any conflicts of interest to disclose.

Code and Data Availability

No code or data were used in the preparation of this manuscript.

Acknowledgments

R.C.L. acknowledges support for this work provided by a National Science Foundation (NSF) Astronomy and Astrophysics Postdoctoral Fellowship (Award No. AST-2102625). This work made use of NASA's Astrophysics Data System Bibliographic Services. This work made use of the NASA/IPAC Extragalactic Database (NED), which is funded by NASA and operated by the California Institute of Technology.

References

1. G. Chin et al., "Single Aperture Large Telescope for Universe Studies (SALTUS): science overview," *J. Astron. Telesc. Instrum. Syst.* **10**(4) (2024).
2. J. W. Arenberg et al., "Design, implementation, and performance of the primary reflector for SALTUS," *J. Astron. Telesc. Instrum. Syst.* **10**(4), 042306 (2024).
3. D. Kim et al., "14-m aperture deployable off-axis far-IR space telescope design for SALTUS observatory," *J. Astron. Telesc. Instrum. Syst.* **10**(4) (2024).
4. L. K. Harding et al., "SALTUS probe class space mission: observatory architecture and mission design," *J. Astron. Telesc. Instrum. Syst.* **10**(4), 042303 (2024).

5. P. Roelfsema et al., "The SAFARI-Lite Imaging Spectrometer for the SALTUS space observatory," *J. Astron. Telesc. Instrum. Syst.* **10**(4) (2024).
6. J. R. G. Silva et al., "The high resolution receiver (HiRX) for the Single Aperture Large Telescope for Universe Studies (SALTUS)," *J. Astron. Telesc. Instrum. Syst.* **10**(4) (2024).
7. J. Spilker et al., "High-redshift extragalactic science with the Single Aperture Large Telescope for Universe Studies (SALTUS) space observatory," *J. Astron. Telesc. Instrum. Syst.* **10**(4), 042305 (2024).
8. K. Schwarz et al., "Star and planet formation science with the Single Aperture Large Telescope for Universe Studies (SALTUS) space observatory," *J. Astron. Telesc. Instrum. Syst.* **10**(4) (2024).
9. C. Anderson et al., "Solar system science with the Single Aperture Large Telescope for Universe Studies space observatory," *J. Astron. Telesc. Instrum. Syst.* **10**(4), 042302 (2024).
10. National Academies of Sciences, *Engineering and medicine, pathways to discovery in astronomy and astrophysics for the 2020s*, The National Academies Press, Washington, DC (2021).
11. M. R. Krumholz, C. F. McKee, and J. Bland-Hawthorn, "Star clusters across cosmic time," *Ann. Rev. Astron. Astrophys.* **57**, 227–303 (2019).
12. G. M. Olivier et al., "Evolution of stellar feedback in H II regions," *Astrophys. J.* **908**, 68 (2021).
13. A. T. Barnes et al., "Comparing the pre-SNe feedback and environmental pressures for 6000 H II regions across 19 nearby spiral galaxies," *Mon. Not. R. Astron. Soc.* **508**, 5362–5389 (2021).
14. B. G. Elmegreen, "On the initial conditions for star formation and the initial mass function," *Astrophys. J.* **731**, 61 (2011).
15. P. F. Hopkins et al., "Galaxies on FIRE (Feedback In Realistic Environments): stellar feedback explains cosmologically inefficient star formation," *Mon. Not. R. Astron. Soc.* **445**, 581–603 (2014).
16. R. C. Kennicutt and N. J. Evans, "Star formation in the Milky Way and nearby galaxies," *Ann. Rev. Astron. Astrophys.* **50**, 531–608 (2012).
17. C. D. Matzner, "On the role of massive stars in the support and destruction of giant molecular clouds," *Astrophys. J.* **566**, 302–314 (2002).
18. S. Geen et al., "Feedback in clouds II: UV photoionization and the first supernova in a massive cloud," *Mon. Not. R. Astron. Soc.* **463**, 3129–3142 (2016).
19. J.-G. Kim, W.-T. Kim, and E. C. Ostriker, "Modeling UV radiation feedback from massive stars. II. Dispersal of star-forming giant molecular clouds by photoionization and radiation pressure," *Astrophys. J.* **859**, 68 (2018).
20. B. G. Elmegreen and C. J. Lada, "Sequential formation of subgroups in OB associations," *Astrophys. J.* **214**, 725–741 (1977).
21. A. Zavagno et al., "Star formation triggered by the galactic H II region RCW 120. First results from the Herschel Space Observatory," *Astron. Astrophys.* **518**, L81 (2010).
22. E. Churchwell et al., "The bubbling galactic disk," *Astrophys. J.* **649**, 759–778 (2006).
23. A. G. G. M. Tielens, *The Physics and Chemistry of the Interstellar Medium*, Cambridge University Press (2005).
24. S. F. Portegies Zwart, S. L. W. McMillan, and M. Gieles, "Young massive star clusters," *Ann. Rev. Astron. Astrophys.* **48**, 431–493 (2010).
25. E. J. Watkins et al., "PHANGS-JWST first results: a statistical view on bubble evolution in NGC 628," *Astrophys. J. Lett.* **944**, L24 (2023).
26. A. T. Barnes et al., "PHANGS-JWST first results: multiwavelength view of feedback-driven bubbles (the phantom voids) across NGC 628," *Astrophys. J. Lett.* **944**, L22 (2023).
27. C.-G. Kim and E. C. Ostriker, "Three-phase interstellar medium in galaxies resolving evolution with star formation and supernova feedback (TIGRESS): algorithms, fiducial model, and convergence," *Astrophys. J.* **846**, 133 (2017).
28. M. Y. Grudić et al., "STARFORGE: towards a comprehensive numerical model of star cluster formation and feedback," *Mon. Not. R. Astron. Soc.* **506**, 2199–2231 (2021).
29. M. Y. Grudić et al., "Great balls of FIRE - I. The formation of star clusters across cosmic time in a Milky Way-mass galaxy," *Mon. Not. R. Astron. Soc.* **519**, 1366–1380 (2023).
30. L. Lancaster et al., "Geometry, dissipation, cooling, and the dynamical evolution of wind-blown bubbles," *Astrophys. J.* **970**, 18 (2024).
31. A. Tielens, *Molecular Astrophysics*, Cambridge University Press (2021).
32. A. G. G. M. Tielens and D. Hollenbach, "Photodissociation regions. I. Basic model," *Astrophys. J.* **291**, 722–746 (1985).
33. D. J. Hollenbach and A. G. G. M. Tielens, "Dense photodissociation regions (PDRs)," *Ann. Rev. Astron. Astrophys.* **35**, 179–216 (1997).
34. C. Joblin et al., "Structure of photodissociation fronts in star-forming regions revealed by Herschel observations of high-J CO emission lines," *Astron. Astrophys.* **615**, A129 (2018).
35. A. Sternberg and A. Dalgarno, "The infrared response of molecular hydrogen gas to ultraviolet radiation: high-density regions," *Astrophys. J.* **338**, 197 (1989).

36. Z. Nagy et al., "Herschel/HIFI spectral line survey of the Orion Bar. Temperature and density differentiation near the PDR surface," *Astron. Astrophys.* **599**, A22 (2017).
37. N. L. Martín-Hernández et al., "ISO spectroscopy of compact H II regions in the Galaxy. II. Ionization and elemental abundances," *Astron. Astrophys.* **381**, 606–627 (2002).
38. J. Kennicutt et al., "SINGS: the SIRTF nearby galaxies survey," *PASP* **115**, 928–952 (2003).
39. J. R. Brauher, D. A. Dale, and G. Helou, "A compendium of far-infrared line and continuum emission for 227 galaxies observed by the infrared space observatory," *Astrophys. J. Suppl.* **178**, 280–301 (2008).
40. J. Kamenetzky et al., "Herschel-SPIRE imaging spectroscopy of molecular gas in M82," *Astrophys. J.* **753**, 70 (2012).
41. A. K. Leroy et al., "PHANGS-ALMA: arcsecond CO(2-1) imaging of nearby star-forming galaxies," *Astrophys. J. Suppl.* **257**, 43 (2021).
42. J. C. Lee et al., "The PHANGS-JWST treasury survey: star formation, feedback, and dust physics at high angular resolution in nearby galaxies," *Astrophys. J. Lett.* **944**, L17 (2023).
43. A. Poglitsch et al., "The photodetector array camera and spectrometer (PACS) on the Herschel Space Observatory," *Astron. Astrophys.* **518**, L2 (2010).
44. C. Fischer et al., "FIFI-LS: the field-imaging far-infrared line spectrometer on SOFIA," *J. Astron. Instrum.* **7**, 1840003 (2018).
45. D. Hollenbach and C. F. McKee, "Molecule formation and infrared emission in fast interstellar shocks. III. Results for J Shocks in molecular clouds," *Astrophys. J.* **342**, 306 (1989).
46. M. J. Kaufman and D. A. Neufeld, "Far-infrared water emission from magnetohydrodynamic shock waves," *Astrophys. J.* **456**, 611 (1996).
47. D. R. Flower and G. Pineau des Forêts, "Characterizing shock waves in molecular outflow sources: the interpretation of Herschel and Spitzer observations of NGC 1333 IRAS 4B," *Mon. Not. R. Astron. Soc.* **436**, 2143–2150 (2013).
48. J. R. Goicoechea et al., "Herschel far-infrared spectral-mapping of Orion BN/KL outflows: spatial distribution of excited CO, H_2O, OH, O, and C in shocked gas," *Astrophys. J.* **799**, 102 (2015).
49. J. Walawender et al., "NGC 1333: a nearby burst of star formation," in *Handbook of Star Forming Regions, Volume I*, B. Reipurth, Ed., Vol. **4**, p. 346, Astronomical Society of the Pacific (2008).
50. P. Padoan et al., "The power spectrum of turbulence in NGC 1333: outflows or large-scale driving?," *Astrophys. J. Lett.* **707**, L153–L157 (2009).
51. J. Bally et al., "The Orion fingers: near-IR adaptive optics imaging of an explosive protostellar outflow," *Astron. Astrophys.* **579**, A130 (2015).
52. A. L. Plunkett et al., "CARMA observations of protostellar outflows in NGC 1333," *Astrophys. J.* **774**, 22 (2013).
53. B. Nisini et al., "Water cooling of shocks in protostellar outflows. Herschel-PACS map of L1157," *Astron. Astrophys.* **518**, L120 (2010).
54. G. Busquet et al., "The CHESS survey of the L1157-B1 bow-shock: high and low excitation water vapor," *Astron. Astrophys.* **561**, A120 (2014).
55. C. Codella et al., "Astrochemistry at work in the L1157-B1 shock: acetaldehyde formation," *Mon. Not. R. Astron. Soc.* **449**, L11–L15 (2015).
56. J. Bally, D. Devine, and B. Reipurth, "A burst of Herbig-Haro flows in NGC 1333," *Astrophys. J. Lett.* **473**, L49 (1996).
57. G. Sandell and L. B. G. Knee, "NGC 1333-protostars, dust shells, and triggered star formation," *Astrophys. J. Lett.* **546**, L49–L52 (2001).
58. C. J. Davis et al., "A shallow though extensive H2 2.122-μm imaging survey of Taurus-Auriga-Perseus - I. NGC 1333, L1455, L1448 and B1," *Mon. Not. R. Astron. Soc.* **387**, 954–968 (2008).
59. H. G. Arce et al., "The COMPLETE survey of outflows in Perseus," *Astrophys. J.* **715**, 1170–1190 (2010).
60. F. Nakamura, S. Takakuwa, and R. Kawabe, "Substellar-mass condensations in prestellar cores," *Astrophys. J. Lett.* **758**, L25 (2012).
61. J. Bally et al., "Outflows, dusty cores, and a burst of star formation in the North America and Pelican Nebulae," *Astronom. J.* **148**, 120 (2014).
62. G. J. Herczeg et al., "Water in star-forming regions with Herschel: highly excited molecular emission from the NGC 1333 IRAS 4B outflow," *Astron. Astrophys.* **540**, A84 (2012).
63. S. Maret et al., "Spitzer mapping of molecular hydrogen pure rotational lines in NGC 1333: a detailed study of feedback in star formation," *Astrophys. J.* **698**, 1244–1260 (2009).
64. E. Tarantino et al., "Characterizing the multiphase origin of [C II] emission in M101 and NGC 6946 with velocity-resolved spectroscopy," *Astrophys. J.* **915**, 92 (2021).
65. M. K. Crawford et al., "Far-infrared spectroscopy of galaxies: the 158 micron C+ line and the energy balance of molecular clouds," *Astrophys. J.* **291**, 755–771 (1985).
66. P. F. Goldsmith et al., "Collisional excitation of the [C II] fine structure transition in interstellar clouds," *Astrophys. J. Suppl.* **203**, 13 (2012).

67. R. Herrera-Camus et al., "SHINING, a survey of far-infrared lines in nearby galaxies. II. Line-deficit models, AGN impact, [C II]-SFR scaling relations, and mass-metallicity relation in (U)LIRGs," *Astrophys. J.* **861**, 95 (2018).
68. K. M. Sandstrom et al., "PHANGS-JWST first results: mapping the 3.3 μm polycyclic aromatic hydrocarbon vibrational band in nearby galaxies with nircam medium bands," *Astrophys. J. Lett.* **944**, L7 (2023).
69. B. G. Elmegreen et al., "Hierarchical star formation in the spiral galaxy NGC 628," *Astrophys. J.* **644**, 879–889 (2006).
70. R. C. Levy et al., "Outflows from super star clusters in the central starburst of NGC 253," *Astrophys. J.* **912**, 4 (2021).
71. R. C. Levy et al., "The morpho-kinematic architecture of super star clusters in the center of NGC 253," *Astrophys. J.* **935**, 19 (2022).
72. R. L. Karim et al., "SOFIA FEEDBACK survey: the pillars of creation in [C II] and molecular lines," *Astronom. J.* **166**, 240 (2023).
73. M. Luisi et al., "Stellar feedback and triggered star formation in the prototypical bubble RCW 120," *Sci. Adv.* **7**, eabe9511 (2021).
74. M. Tiwari et al., "SOFIA FEEDBACK survey: exploring the dynamics of the stellar wind-driven shell of RCW 49," *Astrophys. J.* **914**, 117 (2021).
75. R. Endsley et al., "A JWST/NIRCam study of key contributors to reionization: the star-forming and ionizing properties of UV-faint z 7-8 galaxies," *Mon. Not. R. Astron. Soc.* **524**, 2312–2330 (2023).
76. M. S. Peeples et al., "A budget and accounting of metals at $z \sim 0$: results from the COS-Halos survey," *Astrophys. J.* **786**, 54 (2014).
77. K. B. W. McQuinn et al., "Characterizing the star formation of the low-mass shield galaxies from Hubble Space Telescope imaging," *Astrophys. J.* **802**, 66 (2015).
78. R. J. Bouwens et al., "Reionization era bright emission line survey: selection and characterization of luminous interstellar medium reservoirs in the $z > 6.5$ universe," *Astrophys. J.* **931**, 160 (2022).
79. S. C. Madden et al., "An overview of the Dwarf Galaxy Survey," *Publ. Astron. Soc. Pac.* **125**, 600 (2013).
80. A. O. Benz et al., "Hydrides in young stellar objects: radiation tracers in a protostar-disk-outflow system," *Astron. Astrophys.* **521**, L35 (2010).
81. M. De Luca et al., "Herschel/HIFI discovery of HCl+ in the interstellar medium," *Astrophys. J. Lett.* **751**, L37 (2012).
82. V. Ossenkopf et al., "HIFI observations of warm gas in DR21: shock versus radiative heating," *Astron. Astrophys.* **518**, L79 (2010).
83. S. Martín et al., "ALCHEMI, an ALMA comprehensive high-resolution extragalactic molecular inventory. Survey presentation and first results from the ACA array," *Astron. Astrophys.* **656**, A46 (2021).

Rebecca C. Levy is an NSF astronomy and astrophysics postdoctoral fellow at the University of Arizona. She received her BS degree in astronomy and physics from the University of Arizona in 2015 and her MS degree and PhD in astronomy from the University of Maryland, College Park, in 2017 and 2021, respectively. She has authored more than 40 refereed journal papers. Her research interests include extreme star formation, star clusters, stellar feedback, and the interstellar medium in nearby galaxies using multiwavelength ground- and space-based observations.

Alexander Tielens is a professor of astronomy in the Astronomy Department of the University of Maryland, College Park. He received his master's degree and PhD in astronomy from Leiden University in 1982. He has authored over 500 papers in refereed journals and written two textbooks on the interstellar medium. His scientific interests center on the physics and chemistry of the interstellar medium, particularly in regions of star and planet formation, including the characteristics, origin, and evolution of interstellar polycyclic aromatic hydrocarbon molecules and dust grains. He has published extensively on the radiative and mechanical feedback of massive stars on their environment, especially the observational and theoretical characteristics of photodissociation regions.

Justin Spilker is an assistant professor in the Department of Physics and Astronomy and the Mitchell Institute of Texas A&M University. He is interested in the quenching of galaxies—the processes that prevent galaxies from forming new stars and keep them from forming stars over long timescales. He uses radio/submillimeter interferometers such as ALMA and the VLA for these studies. He has studied a sample of very dusty, highly starforming galaxies detected by the South Pole Telescope that are magnified by a foreground galaxy through gravitational lensing. By virtue of their selection, this sample tends to lie at a higher redshift than other samples observed with either Herschel or SCUBA/SCUBA-2. He has authored about 180 publications.

Daniel P. Marrone is a professor and experimental astrophysicist in the Department of Astronomy/Steward Observatory at the University of Arizona. He received his PhD from Harvard University in 2006. His research addresses galaxies, cosmology, and fundamental physics through a variety of observational tools. He is particularly interested in galaxy clusters and their cosmological applications, galaxy formation in the early universe, and the physics of the supermassive black hole in Sagittarius A*. He has developed new instruments, primarily at centimeter to submillimeter wavelengths. He has authored about 190 publications.

Desika Narayanan is an associate professor of astronomy at the University of Florida and an affiliate of the Cosmic Dawn Center in Copenhagen. He mainly studies the physics of the interstellar medium in galaxies near and far via large-scale numerical simulations of galaxy evolution. He received his BS degree from the University of Florida in 2003 and his PhD from the University of Arizona in 2007. He was the CfA fellow at the Harvard-Smithsonian Center for Astrophysics and the Bok Fellow at the University of Arizona. He was a professor at Haverford College from 2014 to 2017, prior to returning to the University of Florida.

Christopher K. Walker is a professor of astronomy, optical sciences, electrical and computer engineering, aerospace and mechanical engineering, and applied mathematics at the University of Arizona. He received his MSEE from Clemson University in 1980, his MSEE from Ohio State University in 1981, and his PhD in astronomy from the University of Arizona in 1988. He worked at TRW Aerospace and the Jet Propulsion Laboratory, was a Millikan Fellow in Physics at Caltech, and has been a faculty member at the University of Arizona since 1991. He has made many contributions to advance the field of terahertz astronomy. He has supervised sixteen PhD students, led numerous NASA and NSF projects, authored/coauthored 130+ papers, and published two textbooks: “Terahertz Astronomy” and “Investigating Life in the Universe.” He is the principal investigator of the SALTUS mission concept.